Talanta 85 (2011) 2655–2661

Contents lists available at SciVerse ScienceDirect

Talanta

journal homepage: www.elsevier.com/locate/talanta

Determination of silica coating efficiency on metal particles using multiple digestion methods

Jun Wang, Nathan Topham, Chang-Yu Wu*

Department of Environmental Engineering Sciences, University of Florida, Gainesville, FL 32611, USA

ARTICLE INFO

Article history:
Received 19 July 2011
Received in revised form 17 August 2011
Accepted 17 August 2011
Available online 24 August 2011

Keywords:
Metal particles
Silica encapsulation
Coating efficiency
Sample digestion

ABSTRACT

Nano-sized metal particles, including both elemental and oxidized metals, have received significant interest due to their biotoxicity and presence in a wide range of industrial systems. A novel silica technology has been recently explored to minimize the biotoxicity of metal particles by encapsulating them with an amorphous silica shell. In this study, a method to determine silica coating efficiency on metal particles was developed. Metal particles with silica coating were generated using gas metal arc welding (GMAW) process with a silica precursor tetramethylsilane (TMS) added to the shielding gas. Microwave digestion and Inductively Coupled Plasma-Atomic Emission Spectroscopy (ICP-AES) were employed to solubilize the metal content in the particles and analyze the concentration, respectively. Three acid mixtures were tested to acquire the appropriate digestion method targeting at metals and silica coating. Metal recovery efficiencies of different digestion methods were compared through analysis of spiked samples. HNO_3/HF mixture was found to be a more aggressive digestion method for metal particles with silica coating. Aqua regia was able to effectively dissolve metal particles not trapped in the silica shell. Silica coating efficiencies were thus calculated based on the measured concentrations following digestion by HNO_3/HF mixture and aqua regia. The results showed 14–39% of welding fume particles were encapsulated in silica coating under various conditions. This newly developed method could also be used to examine the silica coverage on particles of silica shell/metal core structure in other nanotechnology areas.

1. Introduction

Metal particles, including both elemental and oxidized metals, are commonly found in industrial systems like coal combustor [1], incinerator [2], furnace [3], boiler [4], engine [5], and other high temperature processes involving metals such as arc welding [6]. These metals vaporize at the flame/arc zone, and then quickly nucleate and condense to form nano-sized particles as temperature drops, due to the sharp decrease of their saturation vapor pressure [7]. Those nano-sized metal particles are respirable and able to travel deep within the lung [8]. Compared to their larger size counterparts, nano-sized particles are more likely to penetrate tissues and cannot be easily removed from human body [9]. The presence of toxic metal particles in the ambient and occupational environment has led to a fast development of various control techniques. However, traditional emission control technologies exhibit less effectiveness for those nano-sized metal particles [10]. The tightening of emission standards and occupational exposure limits requires development of next generation control technologies for nano-sized metal particles.

The toxicity of metal particles is mainly decided by their surface composition that is in contact with tissues rather than their bulk composition. A novel amorphous silica technology was recently developed to control nano-sized metal particles and to reduce their toxicity. Silica coating was achieved through the condensation of in situ generated amorphous silica onto metal particles [11,12]. This technology had been demonstrated in several studies of controlling metal particles in flue gas of combustion system [1,13–15]. Amorphous silica has a low solubility in water [16] and is relatively non-toxic compared to metals such as chromium (Cr), manganese (Mn) and nickel (Ni). Hence, amorphous silica coating outside the metal cores has the potential advantage of changing the biotoxicity of metal particles [17]. Recent studies applied this technique to gas tungsten arc welding (GTAW) [18] and gas metal arc welding (GMAW) [19], from which the formed welding fume mainly consisted of nano-sized metal particles. The transmission electron microscopy (TEM) image of fume particles formed with the addition of silica precursor showed some silica shell/metal core particles. However, the silica coating was not present on all the metal particles due to the heterogeneous reaction existing in the welding fume formation. Moreover, different levels of silica coating were found under different shielding gas flow rates. Silica particles alone and uncoated metal particles were also observed in the low shielding gas flow condition. Visual examination by TEM only focused

* Corresponding author. Tel.: +1 352 392 0845; fax: +1 352 392 3076.
E-mail address: cywu@ufl.edu (C.-Y. Wu).

0039-9140/$ – see front matter © 2011 Elsevier B.V. All rights reserved.
doi:10.1016/j.talanta.2011.08.036

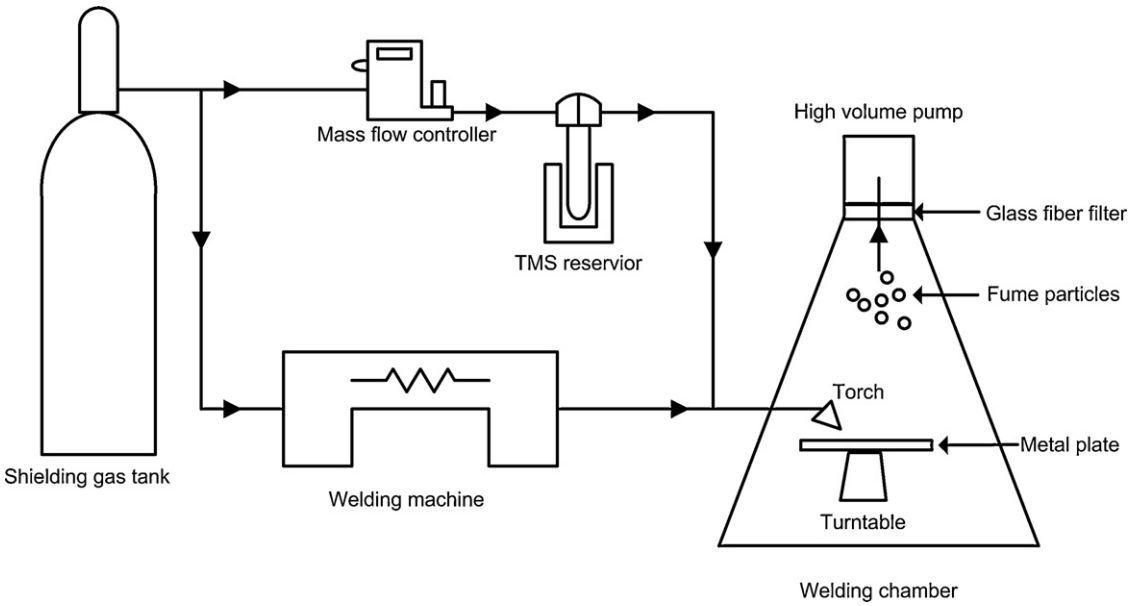

Fig. 1. Schematic diagram for the sampling system.

on a small fraction of the fume particles and cannot be used to quantitatively determine the silica coating efficiency in bulk scale.

Since silica coating efficiency is critical in the silica encapsulation technique, it is necessary to quantify the coating efficiency of silica on metal particles, i.e. the fraction of metals encapsulated inside silica coating that is not bioavailable. Besides metal emission control, it should be noted that silica encapsulation has wide applications in nanotechnology, e.g. to modify the surface function of metal particles [11,12,20–24]. Hence, determination of silica coating efficiencies is important to evaluate the functionality of silica coating in those cases.

Among the analytical systems which can determine the elemental composition of particles, Inductively Coupled Plasma-Atomic Emission Spectroscopy (ICP-AES) is a recognized, versatile analytical instrument for its low detection limit, large dynamic range, and capability of simultaneous analysis of multiple elements [25]. ICP-AES operates on the principle of atomic emission by atoms ionized in argon plasma flame. Light of specific wavelengths is emitted as electrons return to the ground state of the ionized elements and makes it possible to quantitatively identify the species present in the solution [26]. Comparing to Graphite Furnace-Atomic Absorption Spectrometry (GF-AAS) and Proton Induced X-ray Emission (PIXE), ICP-AES has the equivalent detection limit but less matrix effect [27,28]. It costs much less than Inductively Coupled Plasma-Mass Spectroscopy (ICP-MS) [29]. All the above make ICP-AES an inexpensive and relatively accurate way to determine the total metals [30]. However, metal particle samples need to be treated in order to transfer metal analyte from solid phase into liquid solutions. The common practice is to mix particle phase metals with strong acids and dissolve metals in a temperature controlled environment. The digests are diluted to an acceptable total dissolved solids (TDS) concentration for ICP-AES analysis.

Several digestion methods have been reported effective to dissolve metal particles [31–33]. Different digestion methods have varied metal recovery efficiencies. Nitric acid (HNO_3) digestion alone is generally effective for most metals. For certain metals like copper (Cu), recovery efficiency can be greatly promoted by adding hydrofluoric acid (HF) [34]. HF is also commonly employed in digestion of solid samples containing both organic and inorganic silicon [35]. The main concerns for the use of HF are corrosion to silica parts in instrument as well as hazard to operators. This risk can be minimized by adding a stoichiometric amount of boric acid (H_3BO_3) into the complex after digestion. Digestion with aqua regia is also a common method for the determination of trace elements in soils and sediments [36]. Aqua regia is a mixture of nitric acid (HNO_3) and hydrochloric acid (HCl) in a volume ratio of 1:3. There is almost no common metal that can survive the acid attack of aqua regia [37]. Other acids such as sulfuric acid and phosphoric acid were also mentioned in some studies [25,35]. Heating block, ultra-sound assisted and microwave digestions were used to provide a high energetic environment to assist strong acid attack [38,39]. Among those methods, microwave digestion is highly recommended in determination of trace metals with the advantages of fast decomposition rate, less volatile loss, less contamination, precise temperature and pressure control. It requires less acid and therefore can lower the method detection limit [31].

The objective of the study was to develop a method for determining silica coating efficiency on metal particles generated from silica encapsulation technology. Silica coated metal particles were generated using gas metal arc welding (GMAW) with a silica precursor. The fume particles from the process mainly contained Fe, Cr, Ni, Mn, and Cu. Metal recovery efficiencies of three digestion acid mixtures were compared. Silica coating efficiencies were calculated by the apparent concentration differences between digestion methods which can effectively dissolve silica coated metal particles and which can only dissolve metals.

2. Experimental

2.1. Sample preparation

A GMAW welding machine (Lincoln 140C) was used for generating welding fume particles using ER 308L stainless steel welding wires. Fig. 1 shows the schema of the fume production and sampling system. The GMAW welding fume particles primarily come from the welding wire [40]. The 308L welding wire nominally contains 20% Cr, 10% Ni, 1.7% Mn, 0.03% Cu, and balanced with Fe [41]. Silica coated particles were generated by adding tetramethylsilane (TMS) as the silica precursor. Argon and carbon dioxide mixture (3:1, v/v), which is commonly used for stainless steel GMAW, was employed as the shielding gas in this study. A fraction of the shielding gas was used as the carrier gas for the TMS vapor. Injected TMS

Table 1
Welding parameters and silica coating efficiencies under different welding conditions.

Welding condition	Primary shielding gas flow rate (Lpm)	TMS carrier gas flow rate (Lpm)	Silica coating efficiency ± SD (*n*)
1	30	2.8	38.67% ± 6.76% (5)
2	25	2.1	25.76% ± 4.21% (4)
3	20	2.1	13.82% ± 3.79% (5)

decomposed at the high temperature welding arc zone to form an amorphous silica coating on welding fume particles. The particles thus generated were then collected onto glass fiber filter (Whatman, 90 mm), weighed and digested. Previous study showed the higher shielding gas flow rate, the more silica coating observed [19]. Hence, three welding conditions were selected to represent the low, medium, and high shielding gas flow conditions studied previously. The operating parameters of different welding conditions are listed in Table 1. Sampling under each condition was carried out at least four times.

2.2. Instrumentation and chemical reagents

Analysis of total metals was carried out by an ICP-AES system (Perkin-Elmer Plasma 3200). The system is equipped with a plasma torch with an alumina injector which enables measurement of the samples with HF. Two monochromators covering the spectral range of 165–785 nm with a grated ruling of 3600 lines/mm are included in the system. The system also contains a crossflow nebulizer, a spray chamber, and a Gilson four-channel peristaltic pump. The system is capable of analyzing metals in digest solution with a detection limit range of less than part per million (ppm). The operating conditions for the ICP-AES are listed in Table 2.

The metals analyzed by ICP-AES included Fe, Cu, Cr, Ni, and Mn. Two atomic emission spectral lines for each element were used simultaneously to reduce spectral interference introduced by other co-existing elements in the matrix. The wavelengths of their spectral lines are listed in Table 3. The concentration of each metal in a sample was determined by averaging the results of five reading replicates. A single calibration curve was constructed for each metal with six aqueous standards. The concentration ranges of calibration solutions were 10–100 mg L^{-1} for Fe and 1–60 mg L^{-1} for Cr, Ni, Mn, and Cu. All the calibration plots were linear in the investigated concentration ranges with the correlation coefficients greater than 0.99999. Blank samples were used to determine the method detection limits of different digestion methods. Standard samples were randomly inserted into sample queue to test the bias after a relatively long period of running ICP-AES.

Table 2
Operating conditions of Plasma 3200 ICP-AES.

Incident power (W)	1300
Plasma gas flow rate (Lpm)	13
Auxiliary gas flow rate (Lpm)	0.5
Nebulizer gas flow rate (Lpm)	0.8
Peristaltic pump flow rate (mL min^{-1})	1
Reading delay time (s)	40
Reading per sample	5 replicates

Table 3
Wavelength of spectral lines (nm) and method detection limit (mg L^{-1}) for each metal in this study.

Metal	Wavelengths (interference metals [57][a])	Digestion acid mixture		
		HNO_3 alone	HNO_3/HF mixture	Aqua regia
Fe	238.204, 259.940	0.49	0.32	0.36
Cr	205.552 (Fe, Mo), 267.716 (Mn, V)	0.28	0.33	0.29
Ni	231.604, 221.647	1.66	0.57	0.48
Mn	257.610 (Fe, Cr), 293.306 (Fe, Al)	0.66	0.47	0.85
Cu	324.754, 327.396	0.78	0.36	0.54

[a] The potential interference by metals listed cannot be corrected due to the overlap of peak shoulders.

The mass of collected samples was measured by an analytical scale (Sartorius MC210S) with a readability of 10 μg. Each batch of samples was weighed three times and the mean value was calculated. Transmission electron microscopy (TEM, JEOL 2010F) was used to acquire visual evidence of silica coating on welding fume particles. The fume particles were loaded onto a specialty TEM grids (Pelco Lacey Carbon Type-A 300 mesh) inserted into the welding chamber.

All chemicals used were analytical grade or higher purity. Calibration curve was obtained from external standard. Standard solutions were prepared by diluting high purity stock solutions with deionized (DI) water: 10 g L^{-1} Fe and 100 mg L^{-1} Cu (Fisher Scientific), 1000 mg L^{-1} Ni and 1000 mg L^{-1} Mn (Spex Certiprep). Cr standard was in the form of 1000 mg L^{-1} chromate (CrO_4^{2-}) (Acros Organics) and thus conversion was necessary to get the Cr concentration.

$$[\mathrm{Cr}] = [\mathrm{CrO_4^{2-}}]\frac{51.996\ \mathrm{g/mol}}{115.992\ \mathrm{g/mol}} \quad (1)$$

All acid solutions (Fisher Scientific), HNO_3, HF, and HCl were at their original concentration and not diluted. Boric acid (H_3BO_3) (Acros Organics) was obtained in solid phase. Water used for dilution and cleaning was deionized by a water purification system (Barnstead Nanopure II) to a final conductivity of 18.2 mΩ-cm.

Labwares were cleaned before and after analysis to prevent exposure to potential residual contamination during the whole period of experiments. Polytetrafluoroethylene (PTFE) tubes with screw caps (VWR) were used as the digestion vessel to eliminate the risk of HF to glassware. Screw caps can prevent the vaporization of analyte and environmental contamination. All glassware and PTFE tubes were rinsed by DI water, immersed in nitric acid bath (3 M HNO_3) for at least 72 h, cleaned in an ultrasonic cleaner (FS220) for 4 h, and dried in an oven (230G Isotemp) in a laminar flow hood. To further minimize the memory effect of any acid employed in this study, each PTFE tube was labeled and fixed to a specific digestion method, e.g., the tube used for HNO_3 alone and aqua regia will not contact with HF under any circumstances.

2.3. Digestion process

Digestion was assisted by using a microwave digesting system (CEM MDS 81D). An 8-step microwave heating procedure was designed according to the review of experiments done on metal digestion [31] and is listed in Table 4. The sample digests were cooled and filtered by ashless filter (Whatman, 32 mm) to remove the solid residues. The filtered digests were diluted to 50 mL with 2% HNO_3 added. The diluted solutions were analyzed by ICP-AES immediately after dilution.

The basic principle of the digestion process is to utilize HNO_3, HCl, and HF acid to solubilize the metal particles. HNO_3 alone method and aqua regia method were adopted to determine the

Table 4
Operating programs of CEM MDS-81D microwave digesting system.

Increment	Power (W)	Duration (s)
1	250	120
2	400	120
3	500	600
4	250	480
5	400	240
6	600	360
7	0	120
8	300	180

most aggressive acid mixture without breaking the silica coating on metal particles. The particle-loaded filters were cut to quarters after weighing. Each quarter was digested with different acid mixtures. The homogenous mass distribution of metal particles on the filter was examined to avoid interference from mass difference among filter quarters.

HNO_3 alone: Filter samples were placed in the PTFE vessels with 10 mL of HNO_3 added to each vessel. The screw caps on the vessels were tightened to prevent loss during digestion.
HNO_3/HF mixture: HF involved digestion method was based on EPA method 3052 [42] to completely dissolve the metals and silica coating. Filter samples were placed in the PTFE vessels with 9 mL of HNO_3 and 1 mL of HF added to each vessel. After the microwave digestion, a stoichiometric amount of H_3BO_3 was added to eliminate the free fluoride ion in order to prevent damage to the ICP-AES sample loops. The amount of H_3BO_3 was calculated based on the following chemical reaction:

$$H_3BO_3 + 4HF \rightarrow HBF_4 + 3H_2O \quad (2)$$

Aqua regia: Aqua regia (HNO_3:HCl, 1:3, v/v) digestion method was based on ISO standard 11466 [43]. Filter samples were placed in the PTFE vessels with 7.5 mL of HCl and 2.5 mL of HNO_3 added to each vessel.

All the acid mixtures were placed at room temperature for 10 h before sent to the microwave digesting system.

2.4. Method detection limit and recovery efficiency

Blank filters were digested and used as lab blanks to determine the background level of metals. Method detection limit is defined as 3 times standard deviations of metal concentration in lab blank [44]. Relative standard deviation (RSD) was calculated among metals and digestion methods.

The metal recovery efficiency σ was calculated to determine the capacity of each digestion method. Pure metal powders (Acros Organics) were weighed and spiked onto blank glass fiber filters. Measured and known mass of spike samples were compared to calculate the metal recovery efficiency by the following equation.

$$\sigma = \frac{C_{\text{measured}}}{C_{\text{spiked}}} \times 100\% \quad (3)$$

Metal ratios in spiked samples were kept nearly constant and similar to the metal particles generated from the welding process. The spiked samples were digested and analyzed using the same methods as the generated particles. *t*-test was used in comparison of metal recovery efficiency for different digestion methods.

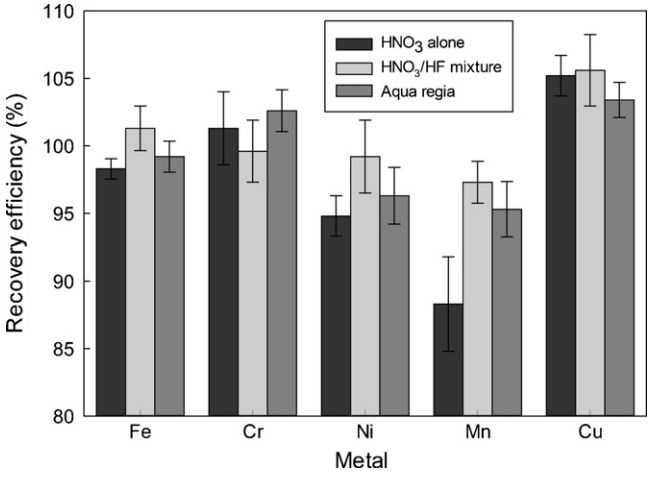

Fig. 2. Recovery efficiencies for Fe, Cr, Ni, Mn, Cu by different digestion acid mixtures.

3. Results and discussion

3.1. Method detection limit

Method detection limits determined from lab blanks are shown in Table 3. Detection limits of five metals in this study were generally around 1 mg L^{-1} level. Based on the results, the choice among different digestion methods had little influence on the method detection limit since the metal concentration in this study is much higher than 1 mg L^{-1}. The HNO_3 alone digestion method shows a slightly better detection limit for Ni and Cu than the other two methods. However, the method detection limits hereby were limited by the instrument (ICP-AES) and trace metal impurity levels of the glass fiber filter. The detection limit could be significantly decreased if analyzed by ICP-MS though it costs more and the procedures are more complicated. The silica shell/metal core structure particles are always synthesized in bulk volume and likely tests will not be carried out for a minute amount of particles. Hence, high resolution (lower than 1 ng L^{-1}) is not necessary in most cases. Glass fiber filter was used in this study because it has good resistance to high temperature generated by welding and it can handle the high flow rate generated by the high-volume sampling pump. Since the trace metal level in glass fibers was much less than the collected metal mass, its impact on method detection limit is not critical to the concentration measurement. In applications where high temperature and high flow rate are not encountered, alternative filters such as cellulose and membrane filters could be used to reduce the trace metal impurities [45–47]. Filters are not necessary if the particles can be transferred to digestion vessel without being collected on filters.

In the experiment, metal matrix effect and HF memory effect could also interfere with the resolution and affect the detection limit [35,48,49]. Carefully acid washing the vessels after the experiment could also lower the detection limit by removing possible residual contaminations.

3.2. Metal recovery efficiency

Fig. 2 shows the recovery efficiencies for different digestion methods and different metals. For all the elements and methods, the recovery efficiencies ranged from 90% to 110%. Recovery efficiencies of HNO_3/HF mixture for all metals except Cu are close to 100% and statistically they are significantly different from the other two methods ($p < 0.05$). Cu has the highest average recovery efficiency of 103.7%. Metal recovery efficiencies over 100% can be attributed to the filter impurity level, e.g., glass fiber filter

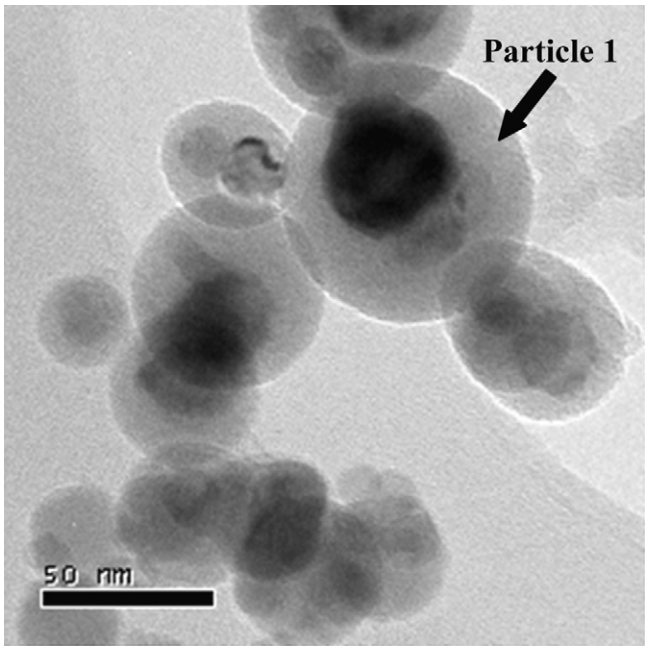

Fig. 3. TEM imaginary of welding fume particles with silica coating.

generally has 3 ng/cm^2 of Cu [46]. The selection of wavelengths of Cr and Mn cannot avoid the spectral inferences from Fe as shown in Table 3. Overestimation of Cr and Mn could happen due to spectral effect induced by high concentration of Fe in the welding fume particles. In addition, non-spectral matrix effect of ICP-AES could either enhance or depress the signals for those metals [49].

The RSD for each metal in different methods was less than 3.5%. Except for Cr, HNO_3/HF mixture showed the highest mean recovery efficiencies compared to the other two acid mixtures ($p < 0.05$). Aqua regia was higher than HNO_3 alone for Mn ($p < 0.05$), but no significant difference was found on other metals. HNO_3 alone showed a low recovery efficiency of 88.3% for Mn and a relatively high deviation. This represents the relatively low acid attack ability by HNO_3 alone. Hence, aqua regia was adopted instead of HNO_3 acid alone in the following silica coating efficiency test to have a comparison with HNO_3/HF mixture. However, mixture of HCl and HNO_3 requires a well sealed vessel such as PTFE tube due to the formation of highly evaporative gas phase NOCl and Cl_2. HNO_3 alone could be an alternative if the sealant cannot be perfectly achieved. In this study, the recovery efficiency test was done using elemental metals, while in real applications such as flame synthesis or welding fume, metal oxides could dominate the particle compositions. Differences in their solubilities should be checked. However, the differences can be neglected in high energy environment provided by the microwave digestion system [50].

3.3. Silica coating efficiency

Fig. 3 shows the TEM imagery of fume particles collected at welding condition 1. Metal particles are darker while silica is in light color, due to the penetration ability of electron when interacting with the particles. In the TEM image, some particles (e.g., Particle 1) have a high electron density (darker) region surrounded by a low electron density region (lighter). This is likely the result of metal encapsulated by the silica coating layer. Nonetheless, due to the two-dimensional nature of TEM image, metal in particle 1 could be non-, partially or fully encapsulated or even enriched on silica surface [51], in a three-dimensional space. To truly determine the level of encapsulation, the silica coating efficiency would be critically important.

HNO_3/HF mixture breaks the silica coating on the metal particles, and according to the metal recovery efficiencies results it had the most aggressive solubilization ability. Aqua regia showed the similar digestion ability on metal-only particles but did not have any effect on particles with silica coating. The mass difference between the results obtained from these two digestion methods was therefore used to calculate the silica coating efficiency using the following equation.

$$\eta = \frac{\sum_{i=1}^{N} C_{NF,i} - \sum_{i=1}^{N} C_{AR,i}}{\sum_{i=1}^{N} C_{NF,i}} \times 100\% \quad (4)$$

η: silica coating efficiency, %
N: number of metals involved
$C_{NF,i}$: measured concentration of the ith metal digested by HNO_3/HF mixture
$C_{AR,i}$: measured concentration of the ith metal digested by aqua regia

Silica coating efficiency η represents the ratio of metals inside the silica coating, which could not be dissolved by aqua regia. It should be noted that the silica coating efficiency for individual metal can be calculated through this equation without summation. However, due to the heterogeneous interaction between silica and metal in this study, the coating process is not targeting at any specific metal. Hence, the silica coating efficiency for individual metal was not calculated. $C_{AR,i}$ can be replaced with metal concentration measured by other acid digestion methods when appropriate, e.g., HNO_3 acid alone without Mn in the system. For specific applications, some rare metals such as Ru, Ta, Os, and Rh can withstand common acid attack such as aqua regia [52]. Under such a circumstance, the equation is not capable of handling those rare metals.

Silica coating efficiencies were acquired from three sets of samples generated under different welding conditions. Mean value and standard deviation of metal concentration were obtained for all the samples and are shown in Table 5. This shows a relatively consistent welding fume particle composition during the experiment. Cu was not detected at most conditions because of the relatively small proportion of Cu in welding wire. The presence of Cu in some of the samples was likely the ablation of welding nozzle tip and shell, rather than the wire. In the samples where Cu was detected, concentration of Cu was close to the method detection limit. Except Cu, other metals showed a good agreement among replicas (RSD <14%). Results of Mn in welding condition 2 and Ni in welding condition 3 suggest more metals have been digested by aqua-regia than HNO_3/HF mixture. These two anomaly values could be attributed by uneven distribution of particles on different quarters of one glass fiber filter.

Based on the metal concentrations acquired and the equation, silica coating efficiencies were calculated and are listed in Table 1. As shown, the silica coating efficiencies were generally low (<40%), due to the heterogeneous nature of gaseous reaction between silica precursor and metals. The highest silica coating efficiency occurred under welding condition 1 which had a higher shielding gas flow rate. The higher shielding gas dispersed more heat generated from the welding arc. Examination of the inner shell of welding nozzle showed a large amount of white silica powder deposited under the low shielding gas flow condition. This confirmed that TMS in the low shielding gas flow condition already decomposed before reaching the effective coating position, because heat was quickly transferred to the welding nozzle area resulting in formation of silica earlier than desired. As shown, the knowledge of silica coating efficiency is very important in understanding the effect of processing conditions (welding parameters) on the process performance (silica coating distribution). By understanding the defect of welding

Table 5
Measured concentrations of metal elements digested by different acid mixtures.

Metals	Welding condition 1 ($n=5$) Concentration ($mg\,L^{-1}$)	Welding condition 2 ($n=4$) Concentration ($mg\,L^{-1}$)	Welding condition 3 ($n=5$) Concentration ($mg\,L^{-1}$)
$C_{NF,Fe}$	56.34 (1.13)	78.79 (8.67)	63.51 (1.91)
$C_{AR,Fe}$	33.28 (3.00)	51.79 (2.07)	59.38 (3.56)
$C_{NF,Cr}$	31.02 (1.55)	45.45 (1.36)	37.19 (2.98)
$C_{AR,Ct}$	28.13 (2.79)	31.33 (2.19)	28.56 (1.71)
$C_{NF,Ni}$	12.82 (0.38)	20.15 (0.81)	13.41 (0.54)
$C_{AR,Ni}$	n.d.	17.43 (1.57)	14.82 (1.78)
$C_{NF,Mn}$	19.73 (0.99)	20.92 (0.84)	17.65 (1.24)
$C_{AR,Mn}$	14.05 (1.83)	22.17 (3.10)	12.33 (1.11)
$C_{NF,Cu}$	3.12 (1.03)	n.d.	1.78 (0.33)
$C_{AR,Cu}$	n.d.	n.d.	n.d.

n.d.: not detected in the samples or lower than method detection limit.
Number in the parentheses indicated the standard deviation among sample replicates.

nozzle under low shielding gas flow condition, a new welding torch should be developed to allow insulation from the heat transfer.

The equation based on multiple digestion methods can be used in examining silica coverage of various silica shell/metal core structure particles applications [53–59]. The silica coating efficiencies in those cases could be an indicator for the effectiveness of the silica shell, e.g., change of functionality, biocompatibility, or colloidal stability by silica shell.

4. Conclusions

ICP-AES and microwave digestion were capable for simultaneous analysis of multiple metals down to $mg\,L^{-1}$ in this study. The accuracy of results was confirmed by metal recovery efficiencies by different digestion methods. HNO_3/HF acid mixture and aqua regia digestion method were both very effective for treatment of ICP-AES analyte. Major metals (Fe) and minor metals (Cr, Mn, Ni, Cu) in welding particles showed good recovery under those two methods.

The calculation of silica coating efficiencies based on the measured mass difference between two digestion methods quantified the metals sealed inside the silica shell. Five metals were tested in this study based on the composition of stainless steel wires used in metal particles generation. More metal speciation should be examined in the future to verify the method's applicability range. It is also possible to apply this analytical method to applications of silica shell/metal core particles, where high silica coating efficiencies were expected from synthesis based on homogenous reaction but no quantitative confirmation yet.

Metals encapsulated by amorphous silica cannot be further extracted by general acid such as HNO_3 or aqua regia. Hence, silica encapsulation is a promising technique to reduce the biotoxicity of metal compounds in nanoparticles. The experimental result showed silica coating efficiency increased with increasing shielding gas flow rate. The low silica coating efficiency under low shielding gas flow rate was due to the premature decomposition of silica precursors. Modification of welding gun structure to overcome this shortage likely will improve the silica coating efficiencies under a wide range of flow rates.

Acknowledgements

The study was made possible under the U.S. Department of Defense through the Environmental Security Technology Certification Program under Grant No. WP-0903. Authors want to thank Particle Engineering Research Center (PERC) and Major Analytical Instrumentation Center (MAIC) at University of Florida for providing the access to ICP-AES and TEM.

References

[1] P. Biswas, T.M. Owens, C.-Y. Wu, J. Aerosol Sci. 26 (1995) S217–S218.
[2] J.-C. Chen, M.-Y. Wey, W.-Y. Ou, Sci. Total Environ. 228 (1999) 67–77.
[3] B.K. Gullett, K. Raghunathan, Energy Fuels 8 (2002) 1068–1076.
[4] W.J. Frederick, A. Ling, H.N. Tran, S.J. Lien, Fuel 83 (2004) 1659–1664.
[5] D.B. Kittelson, W.F. Watts, J.P. Johnson, J. Aerosol Sci. 37 (2006) 913–930.
[6] A.T. Zimmer, P. Biswas, J. Aerosol Sci. 32 (2001) 993–1008.
[7] V. Sethi, P. Biswas, J. Air Waste Manage. Assoc. 40 (1990) 42–46.
[8] G. Oberdörster, V. Stone, K. Donaldson, Nanotoxicology 1 (2007) 2–25.
[9] P. Biswas, C.-Y. Wu, J. Air Waste Manage. Assoc. 55 (2005) 708–746.
[10] S. Kim, M. Harrington, D. Pui, Experimental study of nanoparticles penetration through commercial filter media, in: A.D. Maynard, D.Y.H. Pui (Eds.), Nanotechnology and Occupational Health, Springer, The Netherlands, 2007, pp. 117–125.
[11] B.K. McMillin, P. Biswas, M.R. Zachariah, J. Mater. Res. 11 (1996) 1552–1561.
[12] P. Biswas, C.-Y. Wu, M.R. Zachariah, B. McMillin, J. Mater. Res. 12 (1997) 714–723.
[13] T.M. Owens, P. Biswas, Ind. Eng. Chem. Res. 35 (1996) 792–798.
[14] P. Biswas, M.R. Zachariah, Environ. Sci. Technol. 31 (1997) 2455–2463.
[15] P. Biswas, C.-Y. Wu, J. Air Waste Manage. Assoc. 48 (1998) 113–127.
[16] R.K. Iler, The Chemistry of Silica: Solubility, Polymerization, Colloid and Surface Properties and Biochemistry of Silica, Wiley-Interscience, 1979.
[17] K.-M. Yu, N. Topham, J. Wang, M. Kalivoda, Y. Tseng, C.-Y. Wu, W.-J. Lee, K. Cho, J. Hazard. Mater. 185 (2011) 1587–1591.
[18] N. Topham, M. Kalivoda, Y.-M. Hsu, C.-Y. Wu, S. Oh, K. Cho, J. Aerosol Sci. 41 (2010) 326–330.
[19] N. Topham, J. Wang, M. Kalivoda, J. Huang, K.-M. Yu, Y.-M. Hsu, C.-Y. Wu, S. Oh, K. Cho, K. Paulson, Ann. Occup. Hyg., submitted for publication.
[20] S.R. Hall, S.A. Davis, S. Mann, Langmuir 16 (1999) 1454–1456.
[21] W. Fu, H. Yang, B. Hari, S. Liu, M. Li, G. Zou, Mater. Chem. Phys. 100 (2006) 246–250.
[22] J.M. Rosenholm, J. Zhang, W. Sun, H. Gu, Microporous Mesoporous Mater. 145 (2011) 14–20.
[23] B. Guo, H. Yim, A. Khasanov, J. Stevens, Aerosol Sci. Technol. 44 (2010) 281–291.
[24] O. Niitsoo, A. Couzis, J. Colloid Interface Sci. 354 (2011) 887–890.
[25] S. Wu, Y.-H. Zhao, X. Feng, A. Wittmeier, J. Anal. At. Spectrom. 11 (1996) 287–296.
[26] D. Atanassova, V. Stefanova, E. Russeva, Talanta 47 (1998) 1237–1243.
[27] N. Menzel, P. Schramel, K. Wittmaack, Nucl. Instrum. Meth. Res. B 189 (2002) 94–99.
[28] R. Rubio, J. Huguet, G. Rauret, Water Res. 18 (1984) 423–428.
[29] E. Webb, D. Amarasiriwardena, S. Tauch, E.F. Green, J. Jones, A.H. Goodman, Microchem. J. 81 (2005) 201–208.
[30] I. Boevski, N. Daskalova, I. Havezov, Spectrochim. Acta B 55 (2000) 1643–1657.
[31] K.J. Lamble, S.J. Hill, Analyst 123 (1998) 103R–133R.
[32] A. Okorie, J. Entwistle, J.R. Dean, Talanta 82 (2010) 1421–1425.
[33] V. Sandroni, C.M.M. Smith, A. Donovan, Talanta 60 (2003) 715–723.
[34] E. Ikävalko, T. Laitinen, H. Revitzer, Fresenius J. Anal. Chem. 363 (1999) 314–316.
[35] Y.-H. Xu, A. Iwashita, T. Nakajima, H. Yamashita, H. Takanashi, A. Ohki, Talanta 66 (2005) 58–64.
[36] T. Myöhänen, V. Mäntylahti, K. Koivunen, R. Matilainen, Spectrochim. Acta B 57 (2002) 1681–1688.
[37] T.R. Dulski, A Manual for the Chemical Analysis of Metals, ASTM, West Conshohocken, PA, 1996.
[38] H.M. Kuss, Fresenius J. Anal. Chem. 343 (1992) 788–793.
[39] A.V. Filgueiras, J.L. Capelo, I. Lavilla, C. Bendicho, Talanta 53 (2000) 433–441.
[40] H.R. Castner, C.L. Null, Weld. J. 77 (1998) 223–231.
[41] J.M. Vitek, S.A. David, Metall. Trans. A 18A (7) (1987) 1195–1202.
[42] U.S.E.P.A., U.S. Government Printing Office, Washington, DC, 1996.
[43] ISO, ISO 11466, 1995.
[44] IUPAC, Detection Limit, Compendium of Chemical Terminology, 1997.
[45] R. Dams, K.A. Rahn, J.W. Winchester, Environ. Sci. Technol. 6 (1972) 441–448.
[46] D.R. Scott, W.A. Loseke, L.E. Holboke, R.J. Thompson, Appl. Spectrosc. 30 (1976) 392–405.

[47] H. Sievering, M.J. Dave, P.G. McCoy, K. Walther, Environ. Sci. Technol. 12 (1978) 1435–1437.
[48] S.H. Tan, G. Horlick, J. Anal. At. Spectrom. 2 (1987) 745–763.
[49] J.L. Todoli, L. Gras, V. Hernandis, J. Mora, J. Anal. At. Spectrom. 17 (2002) 142–169.
[50] R.A. Nadkarni, Anal. Chem. 56 (1984) 2233–2237.
[51] A.D. Maynard, Y. Ito, I. Arslan, A.T. Zimmer, N. Browning, A. Nicholls, Aerosol Sci. Technol. 38 (2004) 365–381.
[52] B.D. Craig, D.S. Anderson, Handbook of Corrosion Data, 2nd ed., ASM International, Materials Park, OH, 1995.
[53] L.M. Liz-Marzán, M. Giersig, P. Mulvaney, Langmuir 12 (1996) 4329–4335.
[54] M.A. Correa-Duarte, M. Giersig, L.M. Liz-Marzán, Chem. Phys. Lett. 286 (1998) 497–501.
[55] C. Graf, D.L.J. Vossen, A. Imhof, A. van Blaaderen, Langmuir 19 (2003) 6693–6700.
[56] D.K. Yi, S.T. Selvan, S.S. Lee, G.C. Papaefthymiou, D. Kundaliya, J.Y. Ying, J. Am. Chem. Soc. 127 (2005) 4990–4991.
[57] M. Ohmori, E. Matijevic, J. Colloid Interface Sci. 150 (1992) 594–598.
[58] Y. Lu, Y. Yin, Z.-Y. Li, Y. Xia, Nano Lett. 2 (2002) 785–788.
[59] A. Teleki, M. Suter, P.R. Kidambi, O. Ergeneman, F. Krumeich, B.J. Nelson, S.E. Pratsinis, Chem. Mater. 21 (2009) 2094–2100.